In Quest of Factors That Control the Enantioselective Catalytic Markovnikov Hydroboration/Oxidation of Vinylarenes

Anna M. Segarra,[a] Elias Daura-Oller,[a] Carmen Claver,[a] Josep M. Poblet,[a]
Carles Bo,*[b] and Elena Fernández*[a]

Abstract: This study attempts to rationalise the unpredictable performance of transition metal catalysed asymmetric hydroboration of vinylarenes on varying the precursor of the catalyst from cationic to neutral species, $[M(cod)(L–L)]BF_4$, $[M(\mu\text{-}Cl)(cod)]_2$/(L–L), the metal (M = Rh and Ir), and the hydroborating reagent (catecholborane, pinacolborane). The approaches are based on the agreement between experimental data provided by (*R*)-Binap and (*R*)-Quinap modified catalytic systems and computational data evidenced by DFT calculations and QM/MM strategies. Unprecedentedly high enantiomeric excesses in the hydroboration/oxidation of vinylarenes with both electron-withdrawing substituents ((*R*)-(+)-1-*p*-F-phenylethanol, *ee* up to 92%) and electron-releasing substituents ((*R*)-(+)-1-*p*-MeO-phenylethanol, *ee* up to 98%), can be attributed to a rhodium halide key intermediate.

Keywords: asymmetric catalysis · catecholborane · density functional calculations · hydroboration · pinacolborane

Introduction

Transition metal catalysed asymmetric B–H addition across the carbon–carbon double bond has proved to be an efficient means of preparing enantioselective organometallic B–C products as useful synthetic intermediates.[1] In addition, chiral organoboronate esters can be efficiently converted into interesting functionalised products (HO-C,[2–8] R_2N-C,[9–11] RCO-C[12–13]) with total retention of the configuration; the catalyst can be easily separated from the intermediates before the work up protocol and reused. This makes the asymmetric hydroboration reaction a recyclable process.[14,15] A variety of chiral bidentate P–P, P–S, P–N and P–Se ligands have been developed to induce asymmetry in this reaction but small changes in the ligand structure result in dramatic increases or decreases in *ee*.[16] However, the nature of the chelating ligand is not the only parameter that affects both the regio- and enantioselectivity, the alkene and the temperature reaction also have a considerable effect.[17,18] The fact that small electronic and steric variations can lead to unpredictable differences in the asymmetric B-H addition to vinylarene substrates, in many cases leads to an experimentally frustrating "trial and error" sequence. In this context and based on a previous postulation,[19] we have recently used model systems from spectroscopic postulated key intermediates in the catalytic cycle,[20] to rationalise the role of the steric and electronic features of the ligands and substrates. The difference in the stability of the key intermediates, when comparing Rh complexes modified with Binap, Quinap and Pyphos ligands, agrees with its experimental induced asymmetry. Moreover, some intermolecular interactions, such as π–π stackings, seem to play an important role in the enantiodifferentiation, when the electronic character is modified by substituted styrenes.

To obtain a complete picture of the sensitivity of the hydroboration reaction, we decided to investigate the effect of other related aspects such as the nature of the hydroborating reagent and the metal and the counterion of the catalyst precursor.

Results and Discussion

The role of the hydroborating reagent: The boron atom of the hydroborating reagent must be sufficiently Lewis acidic to be catalytically activated for hydroboration, if we consider the oxidative addition of the borane, as one of the first

---

[a] A. M. Segarra, E. Daura-Oller, Prof. C. Claver, Prof. J. M. Poblet,
Dr. E. Fernández
Departament de Química Física i Inorgànica
Universitat Rovira i Virgili
Pl. Imperial Tàrraco 1, 43005 Tarragona (Spain)
Fax: (+34) 977-559-563
E-mail: elenaf@quimica.urv.es

[b] Dr. C. Bo
Institute of Chemical Research of Catalonia
Avgda. Països Catalans s/n, 43007 Tarragona (Spain)
E-mail: cbo@iciq.es

© 2004 Wiley-VCH Verlag GmbH & Co. KGaA, Weinheim
DOI: 10.1002/chem.200400574

steps in the catalytic cycle. At this point, diorganyloxyboranes $(RO)_2BH$ have an extremely high degree of Lewis acidity, particularly those which are cyclic compounds with five-membered rings.[21] So far, catecholborane has proved to be the most versatile diorganyloxyborane probably because B-H addition to the metal is straightforward and the steric profile of $C_6H_4O_2B$-coordinated to the metal is favorable. However, it still presents several problems; for example, its intrinsic instability and degradation give rise to complex mixtures of highly active species responsible for a number of side reactions during the catalytic hydroboration.[22] To circumvent these difficulties, it has been recommended that freshly redistilled catecholborane or alternative hydroborating reagents be used. Despite the relatively easy synthetic protocol for preparing diorganyloxyboranes from the corresponding diol or diketone and BH_3, only a few have been isolated. They have been qualitatively tested in the reactivity of transition metal-catalysed hydroboration of alkenes, although to the best of our knowledge their influence on enantioselectivity has not been reported yet.[22–24]

The present study expands the scope of the asymmetric hydroboration/oxidation reaction of vinylarenes with pinacolborane, because it is also a diorganyloxyborane with a five membered ring, which is not as unstable or sensitive to moisture as catecholborane. We wanted to determine the extent to which the higher steric demand of pinacolborane could affect both reactivity and selectivity. In general, we found that the $[Rh(cod)\text{-}(R)\text{-}Quinap]BF_4$ catalyst provided slightly higher percentages of the enantioselective Markovnikov alcohol product when catecholborane is used as the hydroborating reagent instead of pinacolborane, (Table 1, entries 1 and 2). This trend is also observed for the hydroboration/oxidation of substituted styrenes, such as electron-rich styrenes (Table 1, entries 3 and 4) and electron-poor styrenes, (Table 1, entries 5 and 6).

A remarkable different catalytic behavior was observed when the chiral ancillary ligand (*R*)-Binap modified the rhodium complex. Our preliminary experiments indicated that, in the presence of pinacolborane, the percentage of the secondary alcohol formed was similar to that of the primary alcohol. Furthermore, the absolute configuration of the product changed when catecholborane was changed for pinacolborane, which also indicate significant structural differences in the enantioselective step, (Table 2, entries 1 and 2). On the basis of these results, we explored the catalytic hydroboration/oxidation reaction of substituted styrenes, and we also observed an attenuation of regioselectivity and a reversal of enantioselectivity, (Table 2). Significantly, for the corresponding *p*-MeO-styrene changes were induced from *ee* values around 60 % on the (*R*)-(+)-*sec*-alcohol with catecholborane to *ee* 38 % on the (*S*)-(−)-*sec*-alcohol with pinacolborane, (Table 2, entries 7 and 8). The variation in the configuration is even greater at low temperatures, where a more constrained metal complex is expected, (Table 2, entries 9 and 10).

The catalytic cycle should be taken into account when the hydroborating reagent on both reactivity and selectivity is to be rationalised. Since the metal complex needs to accommodate both the hydroborating reagent and the alkene, it seems evident that the more crowded the environment is, the lower the reactivity and selectivity towards the secondary alcohol will be. Thus, the comparative void provided by the isoquinoline region in Quinap allows greater tolerance in the accommodation of pinacolborane. The catalytic activity is then similar to that when catecholborane is used, although primary alcohol is also formed in small quantities. Taking into account that Rh-(*R*)-Quinap mainly provides the Markovnikov alcohol product, (Scheme 1, path a), the primary insertion observed in the presence of pinacolborane could be due to a β-H elimination (Scheme 1, path b), followed by a primary reinsertion sequence, (Scheme 1, path c). The pattern is different when catecholborane is involved in the Rh-(*R*)-Quinap catalysed reaction because the reductive elimination of the hindered secondary alkyl complex may proceed at a rate faster than that of β-H elimination, (Scheme 1, paths d, e). Similar observation is extended to the use of catecholborane with Rh-(*R*)-Binap, (Scheme 1, paths j, k). When Rh-(*R*)-Binap and pinacolborane react, the alkylrhodium intermediate presumably undergoes a more facile β-H elimination (Scheme 1, path h), because of the highly sterically congested secondary alkyl complex, after a primary reinsertion sequence, (Scheme 1, path i). However, we can not rule out the possibility of an initial primary insertion of the alkene because of the steric hindrance of the Rh–borane intermediate, followed by reductive elimination which

Table 1. Asymmetric hydroboration/oxidation of vinylarenes towards (*R*)-(+)-*sec*-alcohol catalysed by $[Rh(cod)\text{-}(R)\text{-}Quinap]BF_4$.[a]

Entry	Borane	Substrate	(*R*)-(+)-*sec*-Alcohol	Yield [%]	Branched [%]	*ee*[b] [%]
1	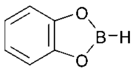	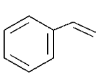	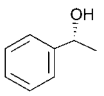	99	95	88
2	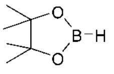			99	75.5	73
3	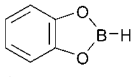	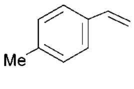	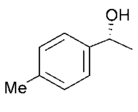	98	97	89
4	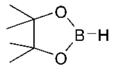			93	91.5	86
5	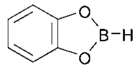	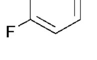	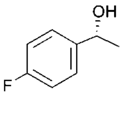	97	96	80
6	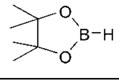			93	93	83

[a] Standard conditions: substrate/borane/Rh complex 1:1.1:0.01. Solvent: THF, $T = 25$ °C, $t = 1$ h. [b] (*R*)-Configuration determined by GC with chiral column FS-Cyclodex B-IP, 50 m × 0.25 mm.

Table 2. Asymmetric hydroboration/oxidation of vinylarenes towards *sec*-alcohol catalysed by [Rh(cod)-(*R*)-Binap]BF_4.[a]

Entry	Borane	Substrate	*sec*-Alcohol	Yield [%]	Branched [%]	*ee*[b] [%]
1	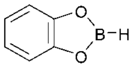	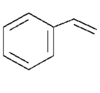	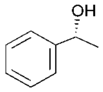	92	99	57(*R*)
2	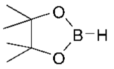		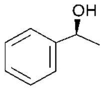	97	50	18(*S*)
3	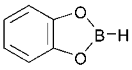	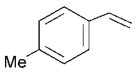	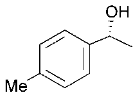	87	99	58(*R*)
4	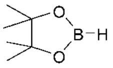		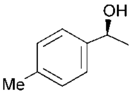	54	41	16(*S*)
5	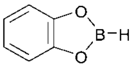	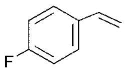	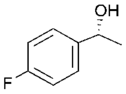	91	99	57(*R*)
6	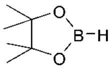		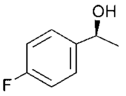	46	46	16(*S*)
7	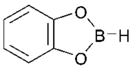	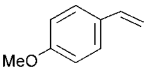	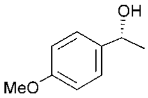	89	99	60(*R*)
8	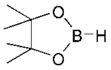		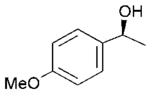	46	58	38(*S*)
9[c]	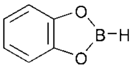		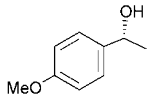	77	99	70(*R*)
10[d]	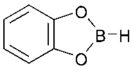			25	99	77(*R*)
11	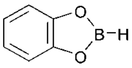	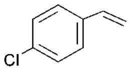	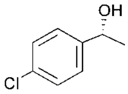	93	99	65(*R*)
12	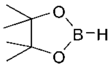		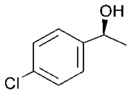	71	45	4(*S*)

[a] Standard conditions: substrate/borane/Rh complex 1:1.1:0.01. Solvent: THF, $T = 25\,^{\circ}C$. $t = 1$ h. [b] Configuration determined by GC with chiral column FS-Cyclodex B-IP, 50 m×0.25 mm. [c] $T = 0\,^{\circ}C$. [d] $T = -78\,^{\circ}C$.

provides the primary product in competition with the favored secondary boronate ester. The moderate reactivity of Rh-(*R*)-Binap/pinacolborane with substituted styrenes, may support this postulation.

As far as the enantioselectivity is concerned, the induced asymmetry in the case of vinylarenes has been previously explained by an intermolecular π–π stacking interaction between the ligand and the substrate. The reversal of enantioselectivity between Rh-(*R*)-Quinap/pinacolborane and Rh-(*R*)-Binap/pinacolborane, may be due to the configuration of the Rh–H fragment when it is transferred to the coordinated alkene. However, a deeper analysis of the data is required. In a previous work,[20] an NMR spectroscopic study of the styrene and catecholborane addition to the precursor of catalyst [Rh(cod)(L–L)]BF_4, where L–L = (*R*)-Binap and (*R*)-Quinap, showed evidence of the structure of the intermediates that may be involved in the asymmetric hydroboration catalytic cycle. From this evidence and using DFT calculations and QM/MM strategies, we studied the origin of regio- and stereoselectivity in the rhodium-catalysed hydroboration reaction of vinylarenes and the role of the steric and electronic features of ligands and substrates. The agreement between the results presented in that work and the experimental trends was excellent. The key intermediate was considered to be the pentacoordinated H-Rh-(P-N)-catecholborane-styrene complex where styrene is coordinated *trans* to the naphthylpyridine moiety and the hydride is in axial position (Figure 1).

We defined two possible isomers according to the position of the hydride: Isomer A when the apex of the square-based pyramid was on the top in Figure 1 and isomer B when it was on the bottom. Each isomer had four possibilities according to the four coordination modes of styrene. In Figure 1, the coordination modes of a monosubstituted alkene are labeled from A1 to A4, and B1 to B4. Notice that four of them lead to linear products (A1 and A2 or B3 and B4), two to a branched pro-S product (A3 or B2) and two to a branched pro-R product (A4 or B1).

Using the same methodology as in our previous study,[20] we considered all eight possible isomers (A1–A4, B1–B4) for the Quinap/styrene/catecholborane and Quinap/styrene/pinacolborane key intermediates and for the Binap analogues. Table 3 shows the relative stability of the most stable isomeric forms (B1 and B2) for the H-Rh-(Quinap)-borane-styrene catalytic system and (B1 and A3) for the H-Rh-(Binap)-borane-styrene system. In the case of Quinap, the difference between *pro-R* B1 and *pro-S* B2 isomers decreased, (from 4.1 to 1.9), when we compared catecholborane and pinacolborane as hydroborating reagents, respec-

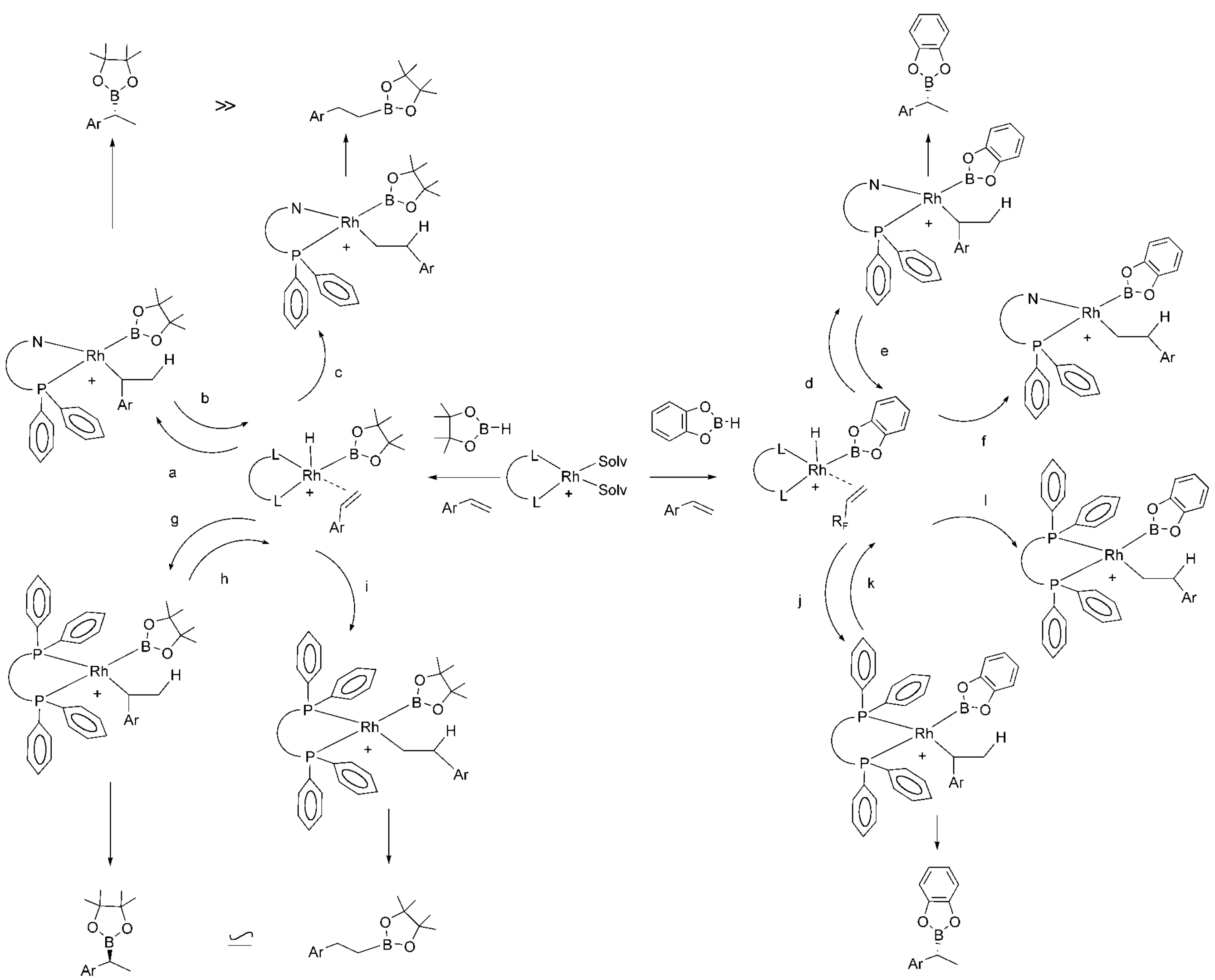

Scheme 1. Plausible catalytic pathways: oxidative addition of the hydroborating reagent to the rhodium complex followed by migratory insertion of the alkene into M–H bond (migratory insertion of the alkene into the M–B bond could also be considered) and reductive elimination.

tively. This result may explain why the *ee* values decreased with this hydroborating agent exchange. In our previous work,[20] we explained the π–π stacking interactions in B1 and B2 H-Rh-(Quinap)-catecholborane-styrene complexes. We showed that the B1 isomer (see Figure 2) was stabilized by π2 interaction and that the B2 isomer was destabilised by π3 an interaction between the substrate and catecholborane, (Figure 2). In the B2 isomer of the H-Rh-(Quinap)-pinacolborane-styrene complex system, we observed a new interaction, known as H(Me)-R^2, (Table 3), between the substrate and one methyl group of the pinacolborane. This kind of stabilising interaction was calculated by Tanabe and coworkers.[25] and in the case of the benzene–ethylene dimer, the equilibrium distance was 3.6 Å. When we changed catecholborane for pinacolborane, B2 was stabilised by this new interaction, H(Me)-R^2. In this respect, the hydroborating agent was responsible for stereoinduction. This is in complete agreement with the experimental decrease in *ee* and the regioselectivity results.

Figure 3 shows the structure obtained for the A3 intermediate in the case of Binap. The results obtained for the two most stable isomers (B1 and A3) are given in Table 3. In the case of H-Rh-(Binap)-catecholborane-styrene, the most stable isomer was the *pro-R* intermediate B1 whereas for the H-Rh-(Binap)-pinacolborane-styrene analogue, the most stable one was the *pro-S* intermediate A3. The accuracy of the computational method to reproduce such small energy differences is obviously questionable, but in any case it is reassuring to be able to reproduce the reversal of enantioselectivity experimentally observed when pinacolborane was used. A detailed analysis of all the interactions of each isomer is far beyond the scope of the present study, but we should point out that slight changes in the catalyst structure modify the interactions which, in turn, determine stereodifferentiation (Figure 4).

The role of the metal: As far as the catalytic system is concerned, the hydroboration reaction is by no means limited

© 2004 Wiley-VCH Verlag GmbH & Co. KGaA, Weinheim

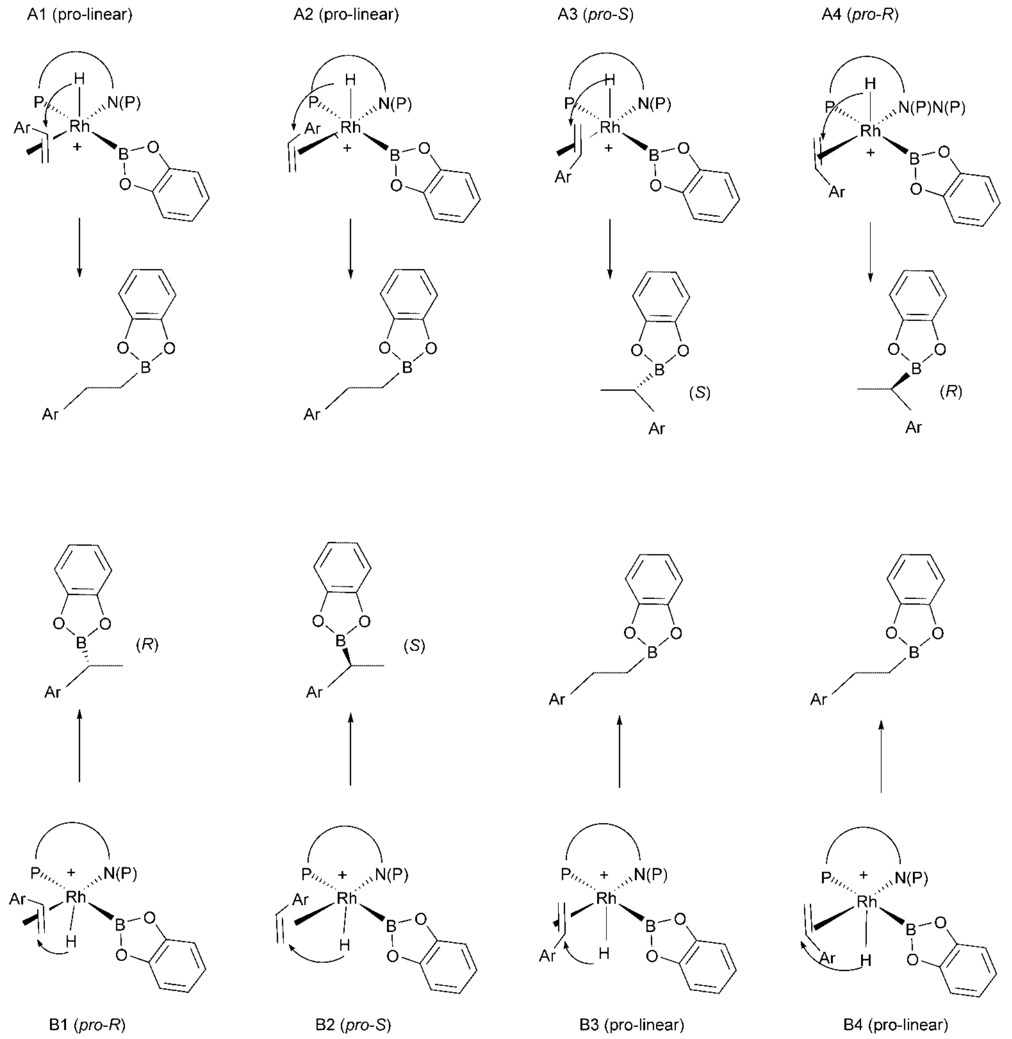

Figure 1.

Table 3. Relative stability and some geometric parameters for the most stable isomeric forms of H-M ligand-borane substrate.[a]

	H-Rh-Quinap-catecholborane-styrene		H-Ir-Quinap-catecholborane-styrene		H-Rh-Quinap-pinacolborane-styrene		H-Rh-Binap-catecholborane-styrene		H-Rh-Binap-pinacolborane-styrene	
	B1	B2	B1	B2	B1	B2	B1	A3	A3	B1
product	(*R*)	(*S*)	(*R*)	(*S*)	(*R*)	(*S*)	(*R*)	(*S*)	(*S*)	(*R*)
relative energy	0.0	4.1	0.0	2.5	0.0	1.9	0.0	0.3	0.0	0.2
distance R^1–R^2	–	3.992	–	4.647	–	–				
distance R^2–R^3	3.555	–	3.560	–	3.410	–				
distance H(Me)–R^2					–	3.125				
angle R^1–R^2	–	36.7	–	33.3						
angle R^2–R^3	24.3	–	24.3	–						
distance R^1–R^4							–	4.604	4.484	–
distance R^1–R^5							5.171	–	–	5.127

[a] Energies in kcal mol^{-1}, distances in Å, angles in degrees.

to rhodium complexes.[26] However, the successful enantioselective transformation of vinylarenes and, to a lesser extent norbornene, has long been restricted to the use of cationic and neutral complexes of this particular transition metal. A recent example of the hydroboration of *meso* substrates in which the enantioselectivity between Rh and Ir systems was

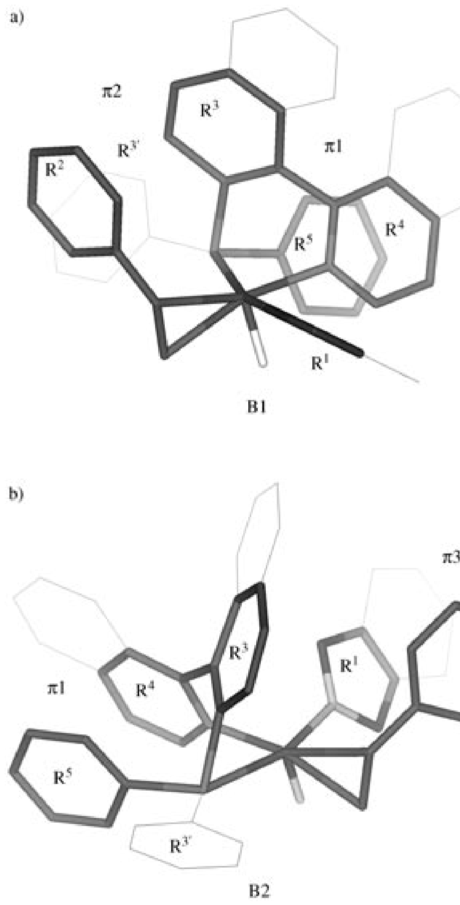

Figure 2. π–π Stacking interactions in the Quinap B1 and B2 isomers. Fragments involved are highlighted. The π^1 occurs between a (R^5) and the pyridine ring (R^4). The π^2 is the interaction between the phenyl styrene (R^2) and the phenyl–P ligand (R^3), and the π^3 corresponds to an interaction between catechoborane (R^1) and phenyl styrene (R^2).

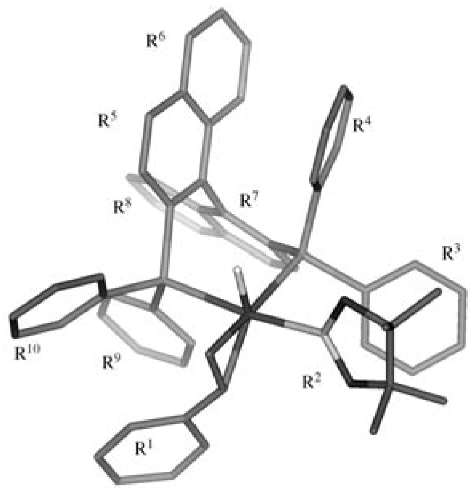

Figure 3. Molecular structure of the H-Rh-Binap-pinacolborane-styrene complex (A3). Hydrogen atoms omitted for clarity.

Table 4. Asymmetric hydroboration/oxidation of styrene towards (*R*)-(+)-1-phenylethanol catalysed by [Ir(cod)-(*R*)-Binap]BF_4.[a]

Catalytic system	Run	Yield [%]	Branched [%]	ee[c] [%]
[Ir(cod)-(*R*)-Binap]BF_4	1	99	30	2
[Ir(cod)-(*R*)-Binap]BF_4/	1	70	17	5
montmorillonite K-10[b]	2	93	31	2

[a] Standard conditions: styrene/catecholborane/Rh complex 1:1.1:0.01. Solvent: THF, $T = 25\,°C$, $t = 1$ h. [b] Montmorillonite K-10 preheated at 100 °C for 24 h, (0.092 mmol [Ir(cod)-(*R*)-Binap]BF_4 per g of solid). [c] (*R*)-Configuration determined by GC with chiral column FS-Cyclodex B-IP, 50 m × 0.25 mm.

completely reversed,[27] led us to wonder whether the Ir-Binap system could also be a suitable catalyst for the hydroboration of vinylarenes. Thus, when the complex [Ir(cod)(*R*)-Binap]BF_4 was used under the same hydroboration reaction conditions as the rhodium system, conversion was complete but enantioselectivity was almost zero and regioselectivity only about 30% on 1-phenylethanol (Table 4. In our ongoing research, we have found that the low enantioselectivity provided by ionic iridium complexes can be improved by immobilising the precursor of the catalyst onto clays. This is the case of [Ir(cod)-(*S*,*S*)-bdpp]PF_6 which efficiently catalyses the hydrogenation of imines such as *N*-(α-methyl-*p*-methoxybenzyl-

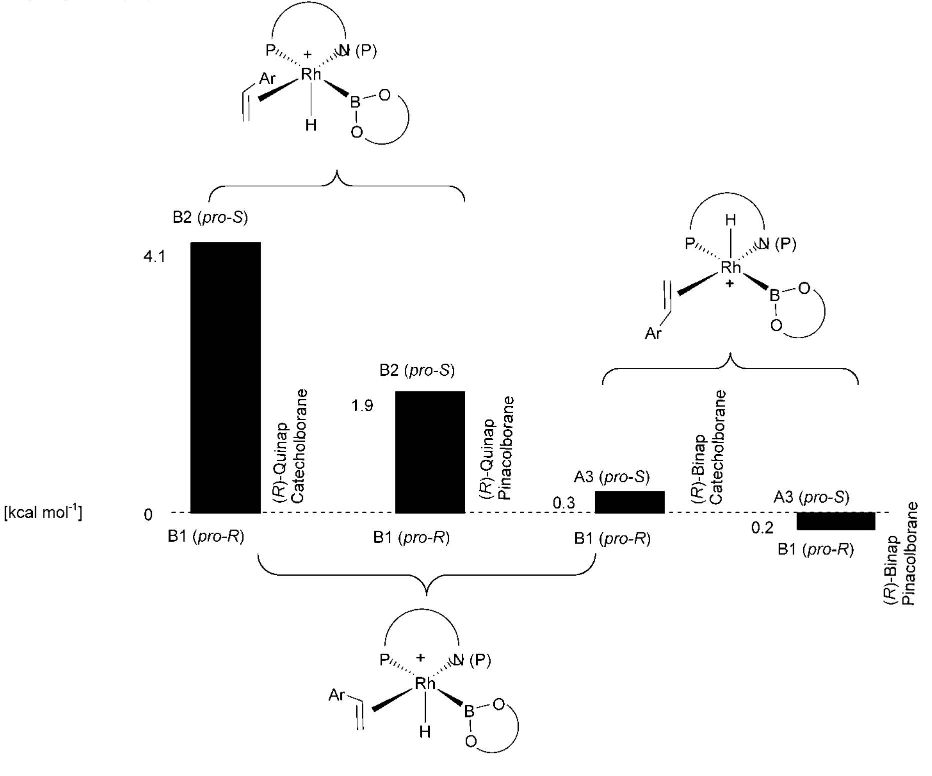

Figure 4.

idene)benzylamine with complete conversion but zero enantiomeric excess, in an homogeneous process. However, when [Ir(cod)-(*S*,*S*)-bdpp]PF_6 was immobilised onto montmorillonite K-10, the catalytic system became more enantioselective on re-use, up to *ee* values around 60% in a third consecutive run.[28] To find a similar effect, we immobilised [Ir(cod)-(*R*)-Binap]BF_4 on montmorillonite K-10, and found that after two consecutive runs the activities and selectivities were similar to those provided by the analogous homogeneous systems (Table 4).

In an attempt to rationalise the low selectivity exhibited by the iridium complexes, we decided to extend our theoretical study to the homogenous catalytic systems [Ir(cod)-(*R*)-Quinap]BF_4. Once again, the question of whether the insertion step or the coordination step in the catalytic cycle are the enantiodifferentiation key steps, is the starting point of discussion. Recently experimental[27] and theoretical studies[29] have proposed two main catalytic cycles that show that the enantiodifferentiation step in the iridium catalysed hydroboration involves the Ir–B migratory insertion step, while the rhodium catalysed hydroboration involves the Rh–H migratory insertion. However, we have calculated a considerable difference in the stability of the isomers when the substrate coordinates to the iridum(I) or rhodium(I) complexes. Table 3 shows how the difference between *pro-R* B1 and *pro-S* B2 isomers decreased when the metal center is iridium and not rhodium. These results explain the low enantiomeric excesses that were observed experimentally. The most significant difference between rhodium and iridium structures was in the B2 isomer, where the π3 π–π stacking distance interaction increased from rhodium (3.992 Å) to iridium (4.647 Å). In our previous study,[20] we made an energetic analysis of the π2 and π3 interactions. For the π3 interaction, the equilibrium distance between ring centroids in a model system was found at 4.6 Å. We demonstrated that, at this distance, the π3 interaction was less repulsive than at the shorter distances found in the rhodium complex. For this reason, in the case of iridium, the B2 isomer is more stable than the rhodium analogue, and the difference in the relative energies of B1 and B2 is lower, (Figure 5). This result is again in good agreement with the observed trends, and shows that a change in the metal center volume can induce changes in the intermolecular interactions, and therefore, changes in *ee* values.

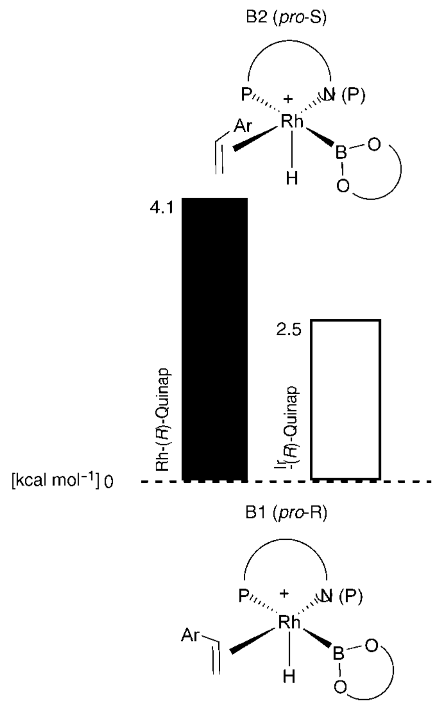

Figure 5.

The role of the halide as counterion: Since both the regio- and the enantioselectivity of the hydroboration of vinylarenes depend heavily on the structural features of the catalysts applied, we found interesting to focus now our study on the nature of the rhodium(I) source with a coordinated and non-coordinated counterion. Thus we carried out a comparative study of the asymmetric hydroboration of vinylarenes with [Rh(cod)-(*R*)-Quinap]BF_4 and [Rh(μ-Cl)(cod)]$_2$/2 equiv (*R*)-Quinap. As in the case of cationic catalysts, we detected a preferentially secondary insertion of styrene into the neutral Rh complex formed from [Rh(μ-Cl)(cod)]$_2$/2 equiv (*R*)-Quinap. However, the neutral catalytic system seems to have an additional influence and favours the enantioselectivity to values up to 94% for the (*R*)-(+)-1-phenylethanol, (Table 5, entries 1 and 2). The scope of the neutral catalytic

Table 5. Asymmetric hydroboration/oxidation of vinylarenes with catecholborane, towards (*R*)-*sec*-alcohol, catalysed by cationic and neutral rhodium complexes.[a]

Entry	Precursor of catalytic system	Substrate	*sec*-Alcohol	Yield [%]	Branched [%]	*ee*[b] [%]
1	[Rh(cod)-(*R*)-Quinap]BF_4	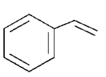	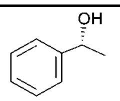 OH	92	95	88
2	[Rh(μ-Cl)(cod)]$_2$/(*R*)Quinap			99	98	94
3	[Rh(cod)-(*R*)-Quinap]BF_4	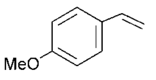 MeO	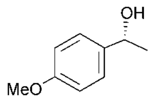 OH MeO	98	96	94
4	[Rh(μ-Cl)(cod)]$_2$/(*R*)-Quinap			92	99	96
5	[Rh(cod)-(*R*)-Quinap]BF_4	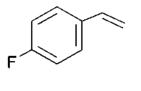 F	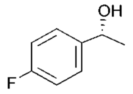 OH F	97	96	80
6	[Rh(μ-Cl)(cod)]$_2$/(*R*)-Quinap			98	98	91.5
7	[Rh(cod)-(*R*)-Quinap]BF_4	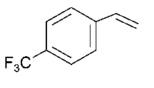 F_3C	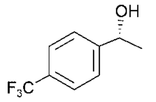 OH F_3C	77	95	38
8	[Rh(μ-Cl)(cod)]$_2$/(*R*)-Quinap			72	90	66

[a] Standard conditions: substrate/borane 1:1.1; cationic complex: 1 mol% [Rh(cod)-(*R*)-Quinap]BF_4; neutral complex: 0.5 mol% [Rh(μ-Cl)(cod)]$_2$/2 equiv (*R*)-Quinap. Solvent: THF, $T = 25\,°C$, $t = 1$ h. [b] Configuration determined by GC with chiral column FS-Cyclodex B-IP, 50 m × 0.25 mm.

© 2004 Wiley-VCH Verlag GmbH & Co. KGaA, Weinheim

system was established for a variety of vinylarenes. In all cases, for styrenes with electron-withdrawing and electron-releasing substituents, the neutral catalytic system increased enantioselectivity to values between 91.5% (*p*-F-styrene) and 96% (*p*-MeO-styrene) (see Table 5, entries 3–6). A clear trend is observed in the hydroboration of the electron deficient vinylarene *p*-CF_3-styrene, where enantioselectivity increases from 38% with the cationic system to 66% with the neutral system. Related literature on the hydroboration of alkenylboronic esters, reports that enantioselectivity was somewhat higher for neutral than for cationic rhodium catalysts, whereas the latter provided better yields.[30] However, no further explanation is given for these facts.

The neutralising influence of chlorine as a coordinated counterion was confirmed in a new experiment where different amounts of the salt $BnMe_3NCl$ were added to the catalytic system [Rh(cod)-(*R*)-Quinap]BF_4, and the products were distributed in a very similar way to when the neutral system was used, (Table 6, entries 1–3). An excess of chlorine did not appear to be necessary. To obtain more information about the role of the halide in the asymmetric hydroboration reaction, we used different additives containing the halide Cl^-, Br^- and I^- in the hydroboration of *p*-F-styrene, (Table 6, entries 4–6). In the three cases, the enantioselectivity increased by the same amount, despite the different electronic and steric factors of the halide. The benefits of having the chloride in the reaction media, in terms of enantioselectivity, can be clearly seen in the hydroboration of *p*-CF_3-styrene and *p*-MeO-styrene, (Table 6, entries 7 and 8). When the substrate was *p*-CF_3-styrene, the *ee* value achieved was 74%, which is only comparable with the asymmetric induction provided by the cationic rhodium complex modified with the closely heterotopic (P,N)-ligand (*S*)-(+)-1-(2-di(2-furyl)phosphino-1-naphthyl)isoquinoline.[17] As far as the substrate *p*-MeO-styrene is concerned, their corresponding secondary alcohol has been obtained with the highest enantiomeric excess reported so far as *ee* 98%.

Table 6. Influence of the halide in asymmetric hydroboration/oxidation of vinylarenes with catecholborane, towards (*R*)-*sec*-alcohol, catalysed by [Rh(cod)-(*R*)-Quinap]BF_4.[a]

Entry	Additive	Substrate	*sec*-alcohol	Yield [%]	Branched [%]	*ee*[b] [%]
1	$BnMe_3NCl$ (0.012 mmol)	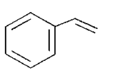	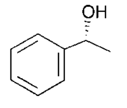	96	95	91
2	$BnMe_3NCl$ (0.03 mmol)			98	96	91.5
3	$BnMe_3NCl$ (0.05 mmol)			94	96	93
4	$BnMe_3NCl$ (0.03 mmol)	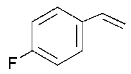	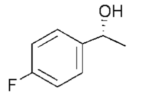	95	95	91.5
5	$PhMe_3NBr$ (0.03 mmol)			85	97.5	92
6	$PhMe_3NI$ (0.03 mmol)			95	95	91.5
7	$BnMe_3NCl$ (0.03 mmol)	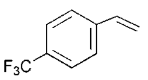	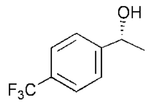	88	97	74
8	$BnMe_3NCl$ (0.03 mmol)	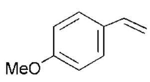	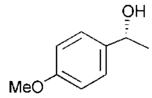	89.5	99	98

[a] Standard conditions: substrate/borane/Rh complex 1:1.1:0.01. Solvent: THF, T = 25°C, t = 1 h. [b] (*R*)-Configuration determined by GC with chiral column FS-Cyclodex B-IP, 50 m × 0.25 mm.

In order to acquire a complete picture of the role of the halide in the asymmetric induction of the hydroboration reaction of vinylarenes, we first attempted to determine which neutral metal species are involved in the first steps of the catalytic cycle. Despite the ambiguities that remain unresolved for the hydroboration catalytic cycle, there is general agreement that the oxidative addition of the hydroborating reagent to the Rh center could be one of the first steps. The first B-H activation from neutral rhodium complexes was observed by Kono and Ito, who isolated the η^1-boryl-rhodium-hydride adduct $[(PPh_3)_2RhClH(B_{cat})]$,[31] (where B_{cat} = catecholborane), from Wilkinson's catalysts, (Figure 6, A). The relative location of the hydride and boryl in these neutral complexes has been confirmed by the complete structural information[32] provided by the analogue complexes $[(PiPr_3)_2RhClH(B_{cat})]$,[33] (where Bcat = catecholborane) and $[(PiPr_3)_2RhClH(B_{pin})]$,[34] (where B_{pin} = pinacolborane), (Figure 6, B). However, to the best of our knowledge, little attention has been paid to the characterisation and structural determination of η^1-boryl-rhodium-hydride intermediates modified with chelating diphosphines. We have recently provided, for first time, spectroscopic evidence of the key intermediate involved in the oxidative addition of catecholborane to the cationic complex [Rh(cod)(L–L)]BF_4 (where L–L = Binap and Quinap).[20] On the basis of this evidence and aimed to extend the factors that govern borane additions to Rh^I centers, we studied the stoichiometric oxidative addition of catecholborane to the neutral catalytic system formed from $[Rh(\mu\text{-}Cl)(cod)]_2$/2 equiv L–L, , (where L–L = Binap and Quinap). For the five coordinate, 16-electron hydride-η^1-boryl-rhodium complex formed, we can expect at least either a square-based pyramid (SP) or a trigonal bipyramid (TBP) geometry. However, the resonances of the hydride ligand were shifted upfield and centered at δ = −15.82 ppm as a double triplet ($J_{H,Rh}$ = 31.2, $J_{H,P}$ = 16.2 Hz) (Figure 7).

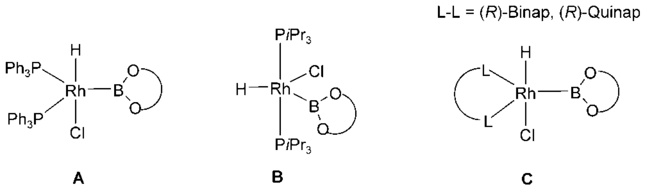

Figure 6.

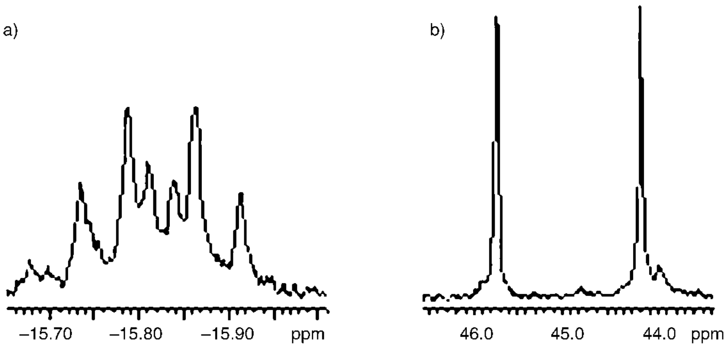

Figure 7. a) Hydride signal in the ^{1}H NMR of complex $[Rh(\mu\text{-}Cl)(cod)]_2$ after the addition of Binap and catecholborane; b) ^{31}P NMR spectrum of the complex $[Rh(\mu\text{-}Cl)(cod)]_2$ after the addition of Binap and catecholborane.

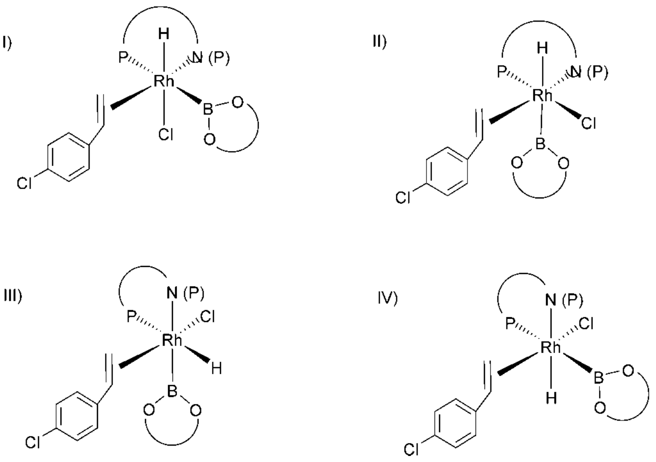

Figure 8. Skeleton of all the hexacoordinated H-Rh-Cl-Quinap-borane-*p*-Cl-styrene isomeric forms considered.

Figure 9. The most stable isomeric form for the H-Rh-Cl-Quinap-borane-*p*-Cl-styrene hexacoordinated complex.

This may indicate that the hydride position is *cis* to two equivalent phosphorous nuclei. The ^{31}P NMR spectrum agrees with the postulated equivalence of the phosphorous nuclei due to the single doublet centered at 44.92 ppm ($J_{P,Rh} = 197.8$ Hz). This oxidative addition was confirmed by ^{11}B NMR spectroscopy, since the initial doublet due to the B bonded to H in free catecholborane ($\delta = 28.8$ ppm, $J_{B,H} = 197.2$ Hz) was shifted to a broad signal centered at $\delta = 23.20$ ppm. The equivalence of the phosphorous in the chelating diphosphine could be indicative of a TBP geometry in which the bidentate ligand is located in the equatorial plane and the hydride ligand occupies the apical position. Since the hydride resonances are chemically shifted upfield and the oxidative addition of catecholborane is expected to be *cis*, we suggest a complete arrangement around the Rh^{III} center, where the halide Cl^- is *trans* to the hydride and the boryl is in the equatorial plane (Figure 6, C). Consistent spectroscopic values are also reported in a related work that describes the oxidative addition of catecholborane to [IrCl(CO)(L–L)] complexes.[35] Taking into account that the following step in the catalytic cycle is the coordination of the alkene to the hydride-η^1-boryl-rhodium intermediate, we can envisage several different isomers with octahedral geometry, which we studied theoretically.

In this section we could not consider the same approximations as in the previous cases because when Cl^- coordinates, the new system presents a hexacoordinated structure. We studied more than twenty different isomeric forms in order to find the most stable structure and to explore much of the configuration space. Figure 8 schematically shows the skeleton of all the intermediates considered here. We first defined isomers in which styrene was *trans* to the naphthyl-pyridine and the hydride *trans* to the Cl^-. Considering the four styrene coordination possibilities and position exchange for hydride and chloride, we took into account eight type I isomers. The second type II also had the styrene *trans* to the naphthyl-pyridine but the Cl^- *cis* to the hydride. The third type III had the styrene *trans* to the Cl^- and the hydride *trans* to the phenyl phosphine moiety and the last type IV had the styrene *trans* to the Cl^- and the hydride *trans* to the naphthyl-pyridine. The most stable form was isomer B1/type III (see Table 7 and Figure 9), the intermediate that leads to the (*R*)-product. The second and third most stable intermediates are those that produce a linear product and the (*S*)-product, respectively. Note that, in general, structural types I and II are less stable than type III and IV, although isomer I/A1 is the second most stable. By splitting the relative energy in its former contribution, QM and MM, the data in Table 7 indicates that the main difference arises from the QM energy, that is, from the part of the molecule that takes into account the differences in the rhodium coordination sphere. In isomer I/A1, a stabilizing MM contribution was computed. A detailed analysis of this geometry suggested that two π-stacking interactions may be present. However, given the small amounts of energy involved and the limitations of the methods used, we think that it is not worthwhile making a detailed analysis of all the interactions in all the isomers. Even so, it should be pointed out that the results obtained using the present computational approach justify, at least qualitatively, the experimentally observed reaction outcome.

Conclusion

Experimentally we found that the efficiency of the hydroborating reagent depends heavily on the steric factors of the

Table 7. Relative stability and some geometric parameters for the most stable isomeric forms of the H-Rh-Cl-Binap-catecholborane-*p*-Cl-styrene system.

Isomer type	Isomer conformation	Hydroborated product	Relative energy	Contribution		Distance R^2–R^3	Distance R^2–$R^{3'}$	Angle R^2–R^3	Angle R^2–$R^{3'}$
				QM	MM				
III	B1	(*R*)	0.0	0.0	0.0	4.490		44.9	
I	A1	linear	2.0	3.3	−1.3	4.735	4.88	28.6	43.4
III	B2	(*S*)	2.3	2.1	0.2	4.854		33.23	
III	B4	linear	2.5	1.2	1.3				
IV	A2	linear	4.1	4.7	−0.6				
I	A3	(*S*)	4.4	5.4	−1.0				
IV	A1	linear	4.4	2.9	1.6				
IV	A4	(*R*)	6.4	3.9	2.6				
III	B3	linear	6.6	3.9	2.7				
IV	A3	(*S*)	6.7	5.1	1.6				
I	B1	(*R*)	7.7	8.5	−0.8				
I	B3	linear	7.8	12.4	−4.6				
I	A4	(*R*)	8.3	6.4	1.9				
I	A2	linear	9.2	7.0	2.2				
II	B3	linear	9.7	18.1	−8.4				
I	B4	linear	12.1	11.7	0.4				
I	B2	(*S*)	12.5	10.9	1.6				
II	A3	(*S*)	17.3	17.5	−0.2				
II	B2	(*S*)	17.9	20.6	−2.7				
II	B4	linear	19.8	22.8	−3.0				
II	B1	(*R*)	20.2	23.5	−3.3				

[a] Energies in $kcal\,mol^{-1}$, distances in Å, angles in degrees. R^2: phenyl styrene, R^3: phenyl–P ligand, $R^{3'}$: phenyl–P ligand.

catalytic systems. So pinacolborane, which is more stable and less sensitive to moisture, can be added to vinylarenes and the selectivities are similar to those for catecholborane, when the catalytic system is based on [Rh(cod)-(*R*)-Quinap]BF_4. Contrary to this trend, a significative reversal in enantioselectivity can be achieved by using pinacolborane or catecholborane with [Rh(cod)-(*R*)-Binap]BF_4.

The consistently high *ee* values observed in the secondary alcohols obtained from the hydroboration/oxidation of vinylarenes with cationic rhodium complexes modified with (*R*)-Quinap, drop sharply to an almost zero asymmetric induction with the related iridium complexes. A significant steric influence must be involved in such different catalytic behavior provided by two catalytic systems that are based on two transition metals with the same d shell electronic configuration.

In addition to the efficiently catalysed hydroboration of vinylarenes by rhodium neutral systems, the enantioselectivity can be significantly enhanced. The coordinated chloride has a positive neutralising effect whether it comes from the catalyst precursor or from an additive such as R_3NCl. Benefits are similar when the nature of the halide is varied from Cl^-, Br^- to I^-. A more in depth analysis was made in an attempt to explain the increase in *ee* values, to as high as 98 % for the hydroboration of *p*-MeO-styrene, which is the highest reported so far in the literature.

From this experimental evidence and applying the same computational approach we used in a previous study,[20] the influence of the nature of the hydroborating reagent, of the metal, and of the counterion can be rationalised. We assumed that the relative stability of the possible isomers is directly related to their population, and that the most stable isomers are those that determine the reaction outcome. Although transition states were not characterised, we found a nice correlation between the experimental findings and isomers stability. For cationic complexes, we previously demonstrated that the present computational approach was able to discriminate ligands and substrates.[20] The results presented here allow extending those conclusions to different hydroborating reagents and to different metals. For neutral complexes, formed by chloride coordination to the catalyst, the scene becomes more complicated since the number of possible conformational isomers is quite high. But also in this case, the most stable structure computed is related to the main product obtained by the experimental procedure.

We expect that those "trial-and-error" approaches could be minimised by using a combination of experiment and theory, as we tried to apply to the hydroboration reaction. Nevertheless, computational modelling of homogeneous catalysis can nowadays complement experimental research in order to increase understanding, but also to provide guides towards rational catalysts design.

Experimental Section

General: All reactions and manipulations were conducted with standard vacuum line techniques under an atmosphere of dry nitrogen. All rhodium and iridium organometallic complexes were synthesised by using standard Schlenk techniques. All organic solvents were purified by standard methods, stored on a molecular sieve (4 Å Aldrich), and degassed with nitrogen flow before use. The complexes $[M(\mu\text{-}Cl)(cod)]_2$,[36] $[M(cod)_2]BF_4$,[37,38] [M(cod)-(*R*)-Binap]BF_4,[39] (where M = Rh, Ir) and [Rh(cod)-(*R*)-Quinap]BF_4,[17] were prepared as previously reported. They were characterised by elemental analysis, ^1H and ^{31}P NMR, and FTIR. Montmorillonite K-10 was purchased from Fluka. Pre-dried montmorillonite K-10 was obtained as follows: 5 g of clay was kept in a melting pot in the oven at 100 °C for 24 h. NMR spectra were recorded on a Varian Gemini 300 and Mercury 400 spectrometer. Chemical shifts were reported relative to tetramethylsilane for ^1H and ^{13}C, 85 % H_3PO_4 for ^{31}P and BF_3OEt_2 for ^{11}B as the external reference. Gas chromatographic analyses were performed on a Hewlett-Packard 5890 II with a flame ionisation detector equipped with a chiral column FS-Cyclodex B-IP, 50 m × 0.25 mm.

Elemental analysis of organometallic complexes was carried out on a Carlo-Erba microanalyzer. IR spectra (range 4000–400 cm^{-1}) were recorded on a FTIR Prospect IR of Midac Corporation spectrometer in KBr pellets.

Homogeneous catalytic hydroboration/oxidation of styrene with catecholborane: Styrene (2 mmol) was added to a solution of catalyst (1 mol %) in THF (2 mL) under nitrogen. The solution was stirred for 5 min and freshly distilled catecholborane (2.2 mmol) was then added. The mixture was stirred at ambient temperature for 1 h and then quenched with EtOH (2 mL). Work up must be carried out carefully because of the risk of explosion by using peroxides with Et_2O and THF. Afterwards, NaOH (2 M, 2 mL) and H_2O_2 (2 mL) were added and the mixture was stirred for several hours. The reaction mixture was extracted into Et_2O, washed (NaOH 2 M, H_2O, saturated brine) dried over $MgSO_4$, and the products characterised by chromatography.

Preparation of the supported complexes: The ionic iridium complexes were immobilised in the following manner. The dichloromethane solutions (5 mL) of complex [Ir(cod)-(*R*)-Binap]BF_4 (0.2 mmol) were prepared under nitrogen and added to a suspension of the solid support Montmorillonite K-10 in deoxygenated dichloromethane (10 mL), and then stirred for 24 h under nitrogen at room temperature. The suspension was filtered off and the solid was washed with dichloromethane and dried under vacuum. The amount of metal complex immobilised on the clay was determined by gravimetric analysis.

Heterogenised catalytic hydroboration/oxidation of styrene: Styrene (2 mmol) was added to a suspension of supported catalyst [Ir(cod)-(*R*)-Binap]BF_4 in montmorillonite K-10, (2 mol % immobilised in 0.5 g of clay), in THF (2 mL) under nitrogen. The solution was stirred for 5 min and freshly distilled catecholborane (2 mmol) was then added. The mixture was stirred at ambient temperature for 2 h. The solution was filtered off under vacuum and the filtrates were then quenched with EtOH (2 mL). The quenched filtrates were treated with NaOH (2 M, 2 mL) and H_2O_2 (2 mL) and the mixture was stirred for several hours. The mixture was finally extracted into Et_2O, washed (NaOH 2 M, H_2O, saturated brine) and dried over $MgSO_4$. The products were then characterised by chromatography. The solid that contained the complex was dried under vacuum for 10 minutes and introduced to the Schlenk for another run.

Computational details: DFT calculations were carried out using the Amsterdam density functional program (ADFv2000) developed by Baerends et al.[40,41]. The numerical integration scheme used in the calculations was developed by te Velde et al.[42,43] and the geometry optimization algorithms implemented by Versluis and Ziegler.[44] The electronic configurations of the molecular systems were described by a triple zeta plus polarization Slater type basis set, as included in the ADF package (basis set IV). The 1s–3d electrons for Rh, the 1s electrons for C, B, O, N and the 2p electrons for P and Cl were treated as frozen cores. Energy differences were calculated by augmenting the local VWN exchange–correlation potential with nonlocal Becke's exchange–correlation correction[45] and Perdew's correlation corrections[46] (BP86). Relativistic effects were considered using the zeroth-order regular approximation (ZORA).[47] No symmetry constraints were used.

For the QM/MM calculations, we applied the IMOMM method[48] as implemented in the ADF package.[49] The QM level we used was the same as the one in the paragraph above. SYBIL[50] force field was used as implemented in ADF to describe the atoms included in the MM part. For the rhodium and boron atom, we used UFF parameters from the literature.[51] The ratio between the P–C(aromatic) bond length and the P–H bond length was 1.234 Å, the ratio between the C(aromatic)–C(aromatic) bond length and the C–H bond length was 1.473 Å and the ratio between the C(aromatic)–C(sp^3) bond length and the C–H bond length was 1.466 Å.

Note Added in Proof

A related report on catalytic hydroboration of vinylarenes with pinacolborane by Cathleen M. Crudden, Yonek B. Hleba and Austin C. Chen, has simultaneously been accepted for publication in *J. Am. Chem. Soc.*

Acknowledgements

The authors are grateful to the Ministerio de Educación y Tecnología for financial support with reference BQU-2002-04110-C02-01 and BQU-2001–0656 and from the CIRIT of the *Generalitat de Catalunya* under Project SGR-1999-00182 and SGR-2001-00316. We thank Ramon Guerrero (NMR techniques) and Jose Carlos Ortiz (computational resources).

---

[1] K. Burgess, M. J. Ohlmeyer, *J. Org. Chem.* **1988**, *53*, 5178–5179.

[2] T. Hayashi, Y. Matsumoto, Y. Ito, *Tetrahedron: Asymmetry* **1991**, *2*, 601–612.

[3] J. M. Brown, D. I. Hulmes, T. P. Layzell, *J. Chem. Soc. Chem. Commun.* **1993**, 1673–1674.

[4] J. M. Valk, G. A. Whitlock, T. P. Layzell, J. M. Brown, *Tetrahedron: Asymmetry* **1995**, *6*, 2593–2596.

[5] A. Schnyder, A. Togni, U. Wiesly, *Organometallics* **1997**, *16*, 255–260.

[6] I. Beletskaya, A. Pelter, *Tetrahedron* **1997**, *53*, 4957–5026.

[7] a) M. McCarthy, M. W. Hooper, P. J. Guiry, *Chem. Commun.* **2000**, 1333–1334; b) M. McCarthy, P. J. Guiry, *Tetrahedron* **2001**, *57*, 3809–3844.

[8] S. Demay, F. Volant, P. Knochel, *Angew. Chem.* **2001**, *113*, 1272–1275; *Angew. Chem. Int. Ed.* **2001**, *40*, 1235–1238.

[9] E. Fernandez, J. M. Brown, *Modern Amination Methods*, VCH, Weinheim, **2000**.

[10] E. Fernandez, K. Maeda, M. W. Hooper, J. M. Brown, *Chem. Eur. J.* **2000**, *6*, 1840–1846.

[11] E. Fernandez, M. W. Hooper, F. I. Knight, J. M. Brown, *Chem. Commun.* **1997**, 173–174.

[12] A. C. Chen, L. Ren, C. M. Crudden, *Chem. Commun.* **1999**, 611–612.

[13] a) L. Ren, C. M. Crudden, *Chem. Commun.* **2000**, 721–722; b) C. M. Crudden, D. Edwards, *Eur. J. Org. Chem.* **2003**, 4695–4712.

[14] A. M. Segarra, R. Guerrero, C. Claver, E. Fernandez, *Chem. Commun.* **2001**, 1808–1809.

[15] A. M. Segarra, R. Guerrero, C. Claver, E. Fernandez, *Chem. Eur. J.* **2003**, *9*, 191–200.

[16] F. Blume, S. Zemolka, T. Fey, R. Kranich, H. G. Schmalz, *Adv. Synth. Catal.* **2002**, *344*, 868–883.

[17] H. Doucet, E. Fernandez, P. T. Layzell, J. M. Brown, *Chem. Eur. J.* **1999**, *5*, 1320–1328.

[18] F. Y. Kwong, Q. Yang, T. C. W. Mak, A. S. C. Chan, K. S. Chan, *J. Org. Chem.* **2002**, *67*, 2769–2777.

[19] J. M Brown, H. Doucet, E. Fernandez, H. E. Heeres, M. W. Hooper, D. I. Hulmes, F. I. Knight, T. P. Layzell, G. C. Lloyd-Jones, *Transition Metal Catalysed Reactions* (Eds.: S. I. Murahashi, S. G. Davies), Blackwell Science, Oxford, **1999**, pp. 465–481.

[20] E. Daura-Oller, A. M. Segarra, J. M. Poblet, C. Claver, E. Fernandez, C. Bo, *J. Org. Chem.* **2004**, *69*, 2669–2680.

[21] A. Lang, H. Nöth, M. Thomann-Albach, *Chem. Ber./Recueil* **1997**, *130*, 363–369.

[22] S. A. Wescott, H. P. Blom, T. B. Marder, R. T. Baker, J. C. Calabrese, *Inorg. Chem.* **1993**, *32*, 2175–2182.

[23] S. Pereira, M. Srebnik, *Organometallics* **1995**, *14*, 3127–3128.

[24] S. Pereira, M. Srebnik, *Tetrahedron Lett.* **1996**, *37*, 3283–3286.

[25] S. Tsuzuki, K. Honda, T. Uchimaru, M. Mikami, K. Tanabe, *J. Am. Chem. Soc.* **2002**, *124*, 104–112.

[26] a) D. Männig, H. Nöth, *Angew. Chem.* **1985**, *97*, 854–855; *Angew. Chem. Int. Ed. Engl.* **1985**, *24*, 878–879; b) D. A. Evans, A. R. Muci, R. Stürmer, *J. Org. Chem.* **1993**, *58*, 5307–5309; c) K. Burgess, M. Jaspers, *Organometallics* **1993**, *12*, 4197–4200; d) K. N. Harrison, T. J. Marks, *J. Am. Chem. Soc.* **1992**, *114*, 9220–9221; e) D. A. Evans, G. C. Fu, *J. Am. Chem. Soc.* **1991**, *113*, 4042–4043;

[27] A. Perez Luna, M. Bonin, L. Micouin, H. Husson, *J. Am. Chem. Soc.* **2002**, *124*, 12098–12099.

[28] R. Margalef-Catala, C. Claver, P. Salagre, E. Fernandez, *Tetrahedron: Asymmetry* **2000**, *11*, 1469–1476.

[29] R. P. Rablen, J. F. Hartwig, S. P. Nolan, *J. Am. Chem. Soc.* **1994**, *116*, 4121–4122.

[30] C. Wiesauer, W. Weissensteiner, *Tetrahedron: Asymmetry* **1996**, *7*, 5–8.

[31] H. Kono, K. Ito, Y. Nagai, *Chem. Lett.* **1975**, 1095–1096.

[32] W. H. Lam, S. Shimada, A. S. Barsanov, Z. Lin, T. B. Marder, J. A. Cowan, J. A. K, Howard, S. A. Mason, G. J. McIntyre, *Organometallics* **2003**, *22*, 4557–4568.

[33] S. A. Westcott, N. J. Taylor, T. B. Marder, R. T. Baker, N. J. Jones, J. C. Calabrese, *J. Chem. Soc. Chem. Commun.* **1991**, 304–305.

[34] S. Shimada, A. S. Batsanov, J. Ak. Howard, T. B. Marder, *Angew. Chem.* **2001**, *113*, 2226–2229; *Angew. Chem. Int. Ed.* **2001**, *40*, 2168–2171.

[35] B. P. Cleary, R. Eisenberg, *Organometallics* **1995**, *14*, 4525–4534.

[36] J. Chatt, L. M. Venanzi, *J. Chem. Soc.* **1957**, 4735–4741.

[37] M. D. Fryzuk, B. Bosnich, *J. Am. Chem. Soc.* **1977**, *99*, 6262–6267.

[38] M. Green, S. H. Kuc, S. H. Taylor, *J. Chem. Soc.* **1971**, 2334–2335.

[39] T. Tani, T. Akutagawa, H. Kumobayashi, T. Taketomi, H. Takaya, A. Miyashita, R. Noyori, S. Otsuka, *J. Am. Chem. Soc.* **1984**, *106*, 5208–5217.

[40] E. J. Baerends, D. E. Ellis, P. Ros, *Chem. Phys.* **1973**, *2*, 41–51.

[41] C. Fonseca Guerra, J. G. Snijders, G. te Velde, E. J. Baerends, *Theor. Chem. Acc.* **1998**, *99*, 391–403.

[42] G. te Velde, E. J. Baerends, *J. Comput. Chem.* **1992**, *13*, 84–98.

[43] P. M. Boerigter, G. te Velde, E. J. Baerends, *Int. J. Quantum Chem.* **1988**, *33*, 87–113.

[44] L. Versluis, T. Ziegler, *J. Chem. Phys.* **1988**, *88*, 322–328.

[45] A. Becke, *Phys. Rev. A* **1988**, *38*, 3098–3100.

[46] a) J. P. Perdew, *Phys. Rev. B* **1986**, *34*, 7406; b) J. P. Perdew, *Phys. Rev. B* **1986**, *33*, 8822–8824.

[47] E. Van Lenthe, A. E. Ehlers, E. J. Baerends, *J. Chem. Phys.* **1999**, *110*, 8943–8953.

[48] a) F. Maseras, K. Morokuma, *J. Comput. Chem.* **1995**, *16*, 1170–1179; b) F. Maseras, *Chem. Commun.* **2000**, 1821–1827.

[49] T. K. Woo, L. Cavallo, T. Ziegler, *Theor. Chem. Acc.* **1998**, *100*, 307–313.

[50] a) M. Clark, R. D. Cramer, N. Van Opdenbosch III, *J. Comput. Chem.* **1989**, *10*, 982–1012; b) U. C. Singh, P. A. Kollman, *J. Comput. Chem.* **1986**, *7*, 718–730.

[51] A. K. Rappé, C. J. Casewit, K. S. Colwell, W. A. Goddard III, W. M. Shiff, *J. Am. Chem. Soc.* **1992**, *114*, 10024–10035.

Received: June 8, 2004
Published online: November 10, 2004

© 2004 Wiley-VCH Verlag GmbH & Co. KGaA, Weinheim